Isoform-Specific Membrane Insertion of Secretory Phospholipase A_2 and Functional Implications†

Abhay H. Pande,‡ Shan Qin,§ Kathleen N. Nemec, Xiaomei He, and Suren A. Tatulian*

Biomolecular Science Center, University of Central Florida, Orlando, Florida 32826

Received May 5, 2006; Revised Manuscript Received July 17, 2006

ABSTRACT: Despite increasing evidence that the membrane-binding mode of interfacial enzymes including the depth of membrane insertion is crucial for their function, the membrane insertion of phospholipase A_2 (PLA_2) enzymes has not been studied systematically. Here, we analyze the membrane insertion of human group IB PLA_2 (hIBPLA$_2$) and compare it with that of a structurally homologous V3W mutant of human group IIA PLA_2 (V3W-hIIAPLA$_2$) and with a structurally divergent group III bee venom PLA_2 (bvPLA$_2$). Increasing the anionic charge of membranes results in a blue shift of the fluorescence of Trp^3 of hIBPLA$_2$, a decrease in quenching by acrylamide, and an increase in enzyme activity, reflecting an enhancement in the membrane binding of PLA_2. Fluorescence quenching by brominated lipids indicates significant penetration of Trp^3 into fluid POPC/POPG membranes but little insertion into the solid DPPC/DPPG membranes. Increased membrane fluidity also supports hIBPLA$_2$ activity, suggesting that membrane insertion of hIBPLA$_2$ is controlled by membrane fluidity and is necessary for the full activity of the enzyme. Trp fluorescence quenching of the V3W-hIIAPLA$_2$ and bvPLA$_2$ by water- and membrane-soluble quenchers indicates substantial membrane insertion of Trp^3 of V3W-hIIAPLA$_2$, similar to that found for hIBPLA$_2$, and no insertion of tryptophans of bvPLA$_2$. Our results provide evidence that (a) structurally similar group IB and IIA PLA_2s, but not structurally diverse group III PLA_2, significantly penetrate into membranes; (b) membrane insertion is controlled by membrane fluidity and facilitates activation of IB and IIA PLA_2s; and (c) structurally distinct PLA_2 isoforms may employ different tactics of substrate accession/product release during lipid hydrolysis.

A myriad of cytosolic and extracellular peripheral membrane proteins bind to target membranes by employing combinations of specific lipid recognition mechanisms and nonspecific physical interactions (*1*, *2*). Recent work has provided evidence that not only the membrane-binding strength but also the precise geometric mode of membrane binding and membrane insertion of peripheral proteins are important determinants of their capabilities to carry out their distinct functions (*3*−*9*). Because of the importance of the orientation and location of membrane proteins with respect to the membrane, this structural feature was referred to as the quinary structure of membrane proteins (*5*, *6*).

Of special interest are the enzymes that acquire their substrates such as lipids of fatty acids from the membrane to which they bind in a process of interfacial activation. Determination of the mode of membrane binding of these enzymes directly contributes to the understanding of important aspects of their function, for example, the mode of substrate acquisition (*10*). On the basis of structural data on group I and III phospholipase A_2 (PLA_2)[1] enzymes from snake and bee venoms, Scott et al. (*11*) suggested that the interface binding surface (IBS) of PLA_2 makes tight contact with the membrane and provides a sealed channel for substrate entrance, thus facilitating optimal enzyme function. The results of EPR experiments indicated that although nonpolar residues of bee venom PLA_2 (bvPLA$_2$) contributed significantly to its membrane binding, the enzyme was bound to the membrane surface without penetration into its hydrocarbon core (*12*). Further biophysical experiments and electrostatic computations suggested that surface dehydration, H-bonding, and p*K* shift effects likely contribute to the peripheral mode of membrane binding of bvPLA$_2$ (*13*).

The IBS of human group IIA PLA_2 (hIIAPLA$_2$) was shown to contain mostly nonpolar as well as cationic amino acid residues, which touched the membrane surface but did not insert into it (*14*), consistent with computational studies

† This work was supported by National Institutes of Health Grant HL65524.

* To whom correspondence should be addressed. Tel: 407-882-2260. Fax: 407-384-2062. E-mail: statulia@mail.ucf.edu.

‡ Present address: Biological Science Group, Birla Institute of Technology and Science, Pilani, India 333031.

§ Present address: Division of Nephrology, Children's Hospital Boston, and Department of Pediatrics, Harvard Medical School, Boston, MA 02115.

[1] Abbreviations: 10-DN, 10-doxylnonadecane; bisPy-PC 1,2-bis-(1-pyrenedecanoyl)-*sn*-glycero-3-phosphocholine; Br_2PC, 1-palmitoyl-2-stearoyl-dibromo-*sn*-glycero-3-phosphocholine; bvPLA$_2$, bee venom phospholipase A_2; DMPC, 1,2-dimyristoyl-*sn*-glycero-3-phosphocholine; DPPC, 1,2-dipalmitoyl-*sn*-glycero-3-phosphocholine; DPPG, 1,2-dipalmitoyl-*sn*-glycero-3-phosphoglycerol; DTPM, 1,2-ditetradecyl-*sn*-glycero-3-phosphomethanol; hIBPLA$_2$, human group IB phospholipase A_2; hIIAPLA$_2$, human group IIA phospholipase A_2; IBS, interface binding surface; LUV, large unilamellar vesicle; N10, the *N*-terminal decapeptide of hIBPLA$_2$; PC, phosphatidylcholine; PLA_2, phospholipase A_2; pIBPLA$_2$, porcine group IB phospholipase A_2; POPC, 1-palmitoyl-2-oleoyl-*sn*-glycero-3-phosphocholine; POPG, 1-palmitoyl-2-oleoyl-*sn*-glycero-3-phosphoglycerol; V3W-hIIAPLA$_2$, the V3W mutant of human group IIA phospholipase A_2.

10.1021/bi060898q CCC: $33.50
Published on Web 00/00/0000

(*15*). Thus, data on bvPLA_2 and hIIAPLA_2 suggested a peripheral mode of PLA_2−membrane interaction without membrane insertion, in agreement with the model of Scott et al. (*11*). However, other workers proposed a partial penetration of the nonpolar side chains of group IB and IIA PLA_2s into the hydrocarbon core of membranes. The immobilization of membrane-partitioned EPR probes upon membrane binding of the porcine group IB PLA_2 (pIBPLA_2) indicated insertion of the nonpolar groups of the enzyme into the membrane (*16*). Molecular dynamics and neutron reflectivity studies also suggested partial membrane insertion of group IA and IIA hIIAPLA_2s (*17*, *18*).

Considerable work has been done to assess the mode of interaction of pIBPLA_2 with phospholipid micelles and membranes (*19*−*21*). Trp^3 fluorescence of pIBPLA_2 in the presence of vesicles composed of phosphatidylcholine (PC), lyso-PC, and brominated stearic acid (100:22:22, molar ratio) was maximally quenched by stearic acid brominated at 11,-12-positions compared to those brominated at 9,10-, 6,7-, or 2-positions (*19*), which would indicate a rather deep insertion of Trp^3 of pIBPLA_2 into membranes. However, the Trp^3 fluorescence could be efficiently quenched by water-soluble succinimide in the presence of vesicles, indicative of a large population of protein with Trp^3 exposed to the aqueous phase (*19*). Further studies showed that the accessibility of water-soluble quenchers, acrylamide and succinimide, to Trp^3 decreased 5−15 times upon binding of pIBPLA_2 to PC micelles (*20*), and when pIBPLA_2 was bound to anionic DTPM vesicles, Trp^3 fluorescence was not affected by these quenchers (*21*). These latter data, together with a maximal fluorescence quenching by11,12-dibromo stearic acid (*19*), strongly suggest significant insertion of pIBPLA_2 into lipid membranes (quenching of Trp^3 by succinimide in the presence of ternary vesicles in ref 19 could result from a substantial fraction of unbound protein in the buffer). However, our recent data on the fluorescence quenching of Trp^3 of human group IB PLA_2 (hIBPLA_2) by brominated lipids indicated that Trp^3 was located at ∼9 Å from the membrane center and, thus, provided support for a deep membrane insertion of group IB PLA_2s (*5*). Despite the evidence contained in these studies, membrane insertion of PLA_2s is not generally recognized, and models of membrane-bound group IB PLA_2s do not involve any appreciable penetration of the protein residues into the membrane (*22*, *23*).

The present work was undertaken in order to analyze the membrane insertion of hIBPLA_2 more comprehensively, to determine its dependence on membrane charge and membrane fluidity, to establish a functional significance of membrane insertion, and to identify the isoform dependence of the membrane insertion of PLA_2s. Our data provide new information indicating that (a) group IB and IIA PLA_2s, but not group III PLA_2, significantly penetrate into membranes; (b) membrane insertion is membrane-charge-independent and fluidity-dependent; (c) membrane insertion facilitates the activity of IB and IIA PLA_2s; and (d) structurally distinct PLA_2 isoforms may employ different tactics of substrate accession/product release during lipid hydrolysis.

MATERIALS AND METHODS

Materials. The lipids 1,2-dipalmitoyl-*sn*-glycero-3-phosphocholine (DPPC), 1,2-dipalmitoyl-*sn*-glycero-3-phosphoglycerol (DPPG), 1-palmitoy-2-oleoyl-*sn*-glycero-3-phosphocholine (POPC), 1-palmitoy-2-oleoyl-*sn*-glycero-3-phosphoglycerol (POPG), and 1-palmitoyl-2-stearoyl-dibromo-*sn*-glycero-3-phosphocholines (Br_2PCs) were purchased from Avanti Polar Lipids (Alabaster, AL); 1,2,bis-(1-pyrenedecanoyl)-*sn*-glycero-3-phosphocholine (bisPy-PC) and 10-doxylnonadecane (10-DN) were from Molecular Probes (Eugene, OR). The sPLA_2 Assay Kit was from Cayman Chemical (Ann Arbor, MI). The *N*-terminal decapeptide of hIBPLA_2 (Ac-Ala-Val-Trp-Gln-Phe-Arg-Lys-Met-Ile-Lys-NH_2) was synthesized by Advanced ChemTech (Louisville, KY) and was ∼99% pure as confirmed by HPLC and mass-spectrometry. The lyophilized PLA_2 purified from honey bee venom was purchased from Sigma-Aldrich (St. Louis, MO). The prokaryotic expression vector for hIBPLA_2 was constructed in this lab, as described (*24*). The pET11a-N1A construct, which harbors the hIIAPLA_2 gene with a N1A mutation, to facilitate removal of the initiator methionine in *E. coli* was a gift from Professor David C. Wilton of the University of Southampton, U.K. The expression plasmid of the V3W mutant of hIIAPLA_2 (V3W-hIIAPLA_2) was constructed on the basis of a pET21a(+) vector, as described in the accompanying article (*25*). Most of the other reagents were purchased from Sigma-Aldrich.

Production and Purification of Proteins. Bee venom PLA_2 was additionally purified by size-exclusion column chromatography using a Bio-Gel P-10 Fine resin (Bio-Rad, Hercules, CA) to obtain a single band in the silver-stained sodium dodecyl sulfate polyacrylamide gel. The protein sample was dialyzed against deionized water using 5 kDa molecular cutoff membranes in order to remove possible low molecular weight contaminations. The hIBPLA_2 and the V3W-hIIA-PLA_2 were expressed in *E. coli* BL21(DE3) and purified, as described (*24*, *25*). All PLA_2 samples were pure, as confirmed by silver-stained gels, were correctly folded into native structures, as confirmed by circular dichroism and activity data, and maintained the structural features and activity over a period of up to one year when lyophilized and stored at −80 °C.

PLA_2 Activity Assay. PLA_2 activity was measured by a fluorescence assay, using phospholipid vesicles labeled with 5 mol % bisPy-PC, as described in the accompanying article (*25*). Large unilamellar vesicles (LUVs) were prepared by extrusion of the lipid suspension through 100 nm pore-size polycarbonate membranes, using a Liposofast extruder (Avestin, Ottawa, Canada), as described (*24*). The total lipid concentration in the suspension was 0.5 mM. In case of lipids that are in the gel (solid) phase at room temperature, such as DPPC and DPPG, the lipid suspension was heated to 55 °C and vortexed to prepare multilamellar liposomes, which were extruded with the extruder immersed in water heated to ∼55 °C in a large beaker. The suspension was then incubated at 25 °C to yield LUVs with membranes in the gel phase. The LUVs for the PLA_2 activity assay were prepared in a buffer containing 50 mM NaCl, 4 mM $CaCl_2$, and 50 mM Hepes (pH 7.4). Fluorescence spectra were measured using a J-810 spectrofluoropolarimeter (Jasco Co., Tokyo, Japan), which is a spectropolarimeter equipped with a Peltier temperature controller and an additional photomultiplier tube mounted at 90° for fluorescence measurements. After recording an initial fluorescence emission spectrum between 370 and 490 nm, using excitation at 347 nm, lipid

hydrolysis was initiated by adding PLA_2 to the LUVs. The emission spectrum of monomeric pyrene contains two peaks at 380 and 396 nm, and the close proximity of pyrene moieties results in an excimer peak at 470 nm (*26*). Hydrolysis of bisPy-PC by PLA_2 separates the two acyl chains of the lipid, each of which has a pyrene moiety, resulting in an increase in the monomer/excimer signal ratio. This effect was used to determine PLA_2 activity as $R_t/R_0 - 1$, where R_t is the ratio of fluorescence intensities at 380 and 470 nm at time t, $R_t = (F_{380}/F_{470})_t$, and R_0 is the same ratio before the addition of PLA_2.

Fluorescence Experiments. Membrane insertion of PLA_2 molecules or the *N*-terminal peptide was determined by fluorescence spectroscopy, using the J-810 spectrofluoropolarimeter described above. The samples were contained in a 4×4 mm^2 rectangular quartz cuvette with constant stirring. Excitation and emission slits were 4 and 10 nm, respectively. Tryptophans were selectively excited at 290 nm, and the emission spectra were recorded between 300 and 400 nm, followed by spectral correction by subtracting the spectra measured under identical conditions but without the protein or peptide. In experiments of Trp fluorescence quenching with acrylamide, PLA_2, or peptide solutions were prepared in buffers that contained 1 mM EDTA and 50 mM Hepes (pH 7.4) and varying concentrations of acrylamide, emission spectra were measured, maximum fluorescence intensities without and with the quencher (F_0 and F respectively) were determined, and F_0/F values were plotted against the acrylamide concentration. The slopes of the best-fit linear plots were used to determine the Stern−Volmer quenching constants (K_{SV}). The experimental data were fitted with the Stern−Volmer equation (*26*)

$$\frac{F_0}{F} = 1 + K_{SV}[Q] \tag{1}$$

where [Q] is the quencher concentration. The total concentration of the lipid was 0.5 mM.

In dual quenching experiments, Trp emission intensity was measured in the presence of lipid vesicles with no quencher (F_0), in the presence of vesicles and with 250 mM acrylamide in the buffer (F_{acryl}), and in the presence of vesicles containing 10 mol % 10-DN with no acrylamide in the buffer (F_{10-DN}). The dual quenching ratio, R_{DQ}, was determined as described earlier (*27*, *28*).

$$R_{DQ} = \frac{F_0/F_{acryl} - 1}{F_0/F_{10-DN} - 1} \tag{2}$$

Values of $R_{DQ} < 1$ indicate that the fluorophore is efficiently shielded from the aqueous phase by membrane insertion, whereas exposure of the fluorophore to the aqueous phase yields $R_{DQ} \gg 1$.

The depth of membrane insertion was quantitatively determined by using differential quenching of Trp fluorescence by Br_2PCs brominated at 6,7-, 9,10-, or 11,12-positions of the *sn*-2 acyl chain. Br_2PCs were incorporated in vesicles at 20 mol %. Initially, Trp fluorescence spectra of the protein or the peptide were measured in the presence of lipid vesicles composed of POPC and POPG, and the emission intensity at 350 nm was measured and designated as F_0. Then, Trp emission intensities at 350 nm (F) were measured in the presence of vesicles in which 20 mol % of POPC was replaced by each of the three Br_2PCs. The values of $\ln(F_0/F)$ were calculated and plotted against the distance of the bromine atoms from the membrane center, that is, 11.0, 8.3, and 6.5 Å for 6,7-, 9,10-, and 11,12-Br_2PCs, respectively (*29*, *30*). The experimental data were described using the following distribution analysis (*30*, *31*).

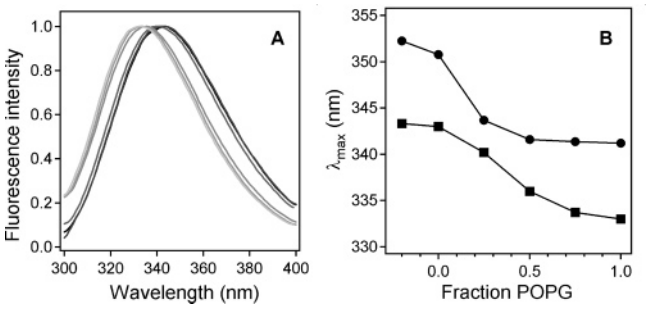

FIGURE 1: Tryptophan fluorescence spectra of $hIBPLA_2$ and the N10 peptide undergo blue shift with increasing fractions of anionic lipid in membranes. (A) Fluorescence spectra of $hIBPLA_2$ in the absence (dotted line, which can be hardly discerned because of overlap with the dark solid line) and presence of lipid vesicles composed of POPC and POPG. The POPG mole fractions in vesicles are 0.0, 0.25, 0.5, 0.75, and 1.0 (solid lines changing from dark to light). The samples were in a buffer of 50 mM Hepes (pH 7.4) and 1 mM EDTA, containing 0.5 mM total lipid and 4 μM PLA_2. Excitation was at 290 nm, and the temperature was 25 °C. (B) Dependence of the peak wavelength (λ_{max}) of fluorescence spectra of $hIBPLA_2$ (■) and the N10 peptide (●) on a fraction of POPG in POPC/POPG membranes. Data for the N10 peptide were obtained under conditions identical to those for $hIBPLA_2$. The data points at the left of the zero fraction POPG correspond to the absence of lipid.

$$\ln\frac{F_0}{F} = \frac{S}{\sigma\sqrt{2\pi}} \exp\left[-\frac{(h - h_m)^2}{2\sigma^2}\right] \tag{3}$$

In eq 3, S is the area under the distribution curve and is directly proportional to the degree of the exposure of the fluorophore to the membrane hydrocarbon core, σ is the dispersion of the distribution curve and is determined by the sizes of the fluorophore and the quencher as well as by the structural disorder and heterogeneity of the system, h is the distance from the membrane center, and h_m is the most probable location of the fluorophore with respect to the membrane center.

RESULTS

Membrane Anionic Surface Charge Facilitates Membrane Recruitment and Activity of hIBPLA$_2$. To assess changes in the microenvironment of the single Trp[3] of $hIBPLA_2$ during membrane binding, Trp fluorescence spectra were measured in the absence and presence of lipid vesicles composed of POPC and POPG with POPG mole fraction (x_{POPG}) changing from zero to one. With pure POPC vesicles, there was little change in the peak position of fluorescence compared with that of the free protein in buffer (Figure 1), indicating that $hIBPLA_2$ does not bind appreciably to zwitterionic membranes. With increasing x_{POPG}, the peak fluorescence wavelength (λ_{max}) decreased in a sigmoidal manner as a function of x_{POPG}. This effect apparently results from the binding of $hIBPLA_2$ to negatively charged membranes, accompanied with either a transfer of Trp[3] from the polar aqueous phase

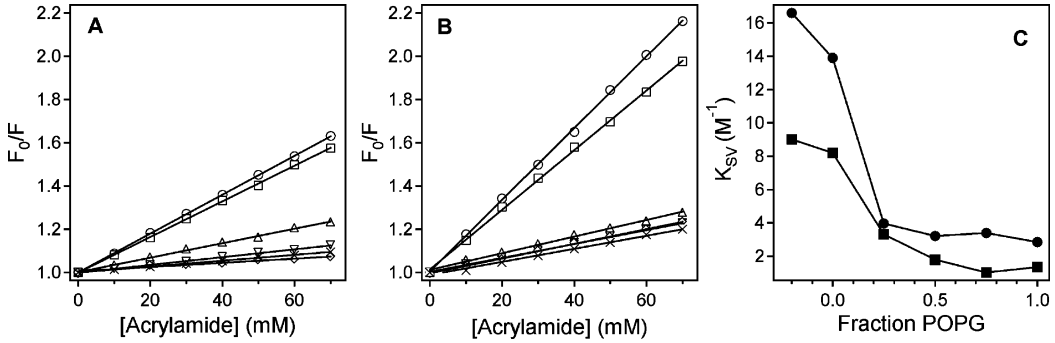

FIGURE 2: Quenching of Trp fluorescence of hIBPLA$_2$ (A) and the N10 peptide (B) by acrylamide in the absence of lipid (○) or in the presence of POPC/POPG vesicles. The mole fraction of POPG in membranes was 0 (□), 0.25 (△), 0.5 (▽), 0.75 (◊), and 1.0 (×). Conditions are the same as those in Figure 1. F_0 and F are maximum fluorescence emission intensities without and with the quencher, respectively. The slopes of the best-fit linear plots have been used to determine the Stern−Volmer quenching constants, K_{SV}. (C) Plots of K_{SV} as a function of a mole fraction of POPG in POPC/POPG membranes for hIBPLA$_2$ (■) and the N10 peptide (●). The data points at the left of the zero fraction POPG correspond to the absence of lipid.

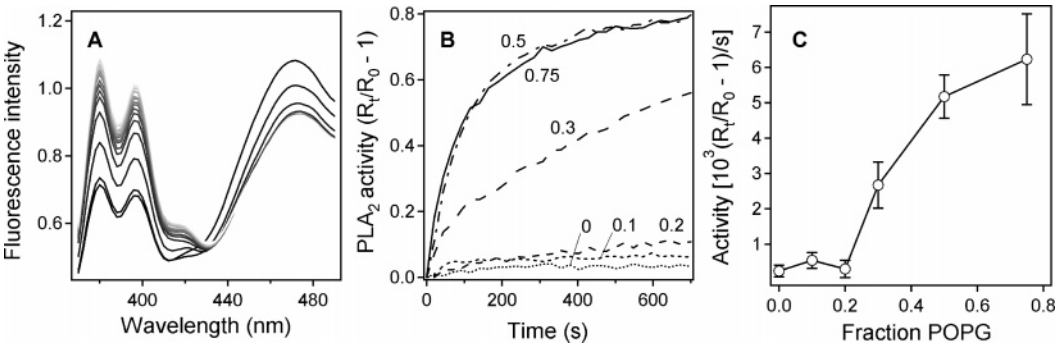

FIGURE 3: Dependence of hIBPLA$_2$ activity on the fraction of anionic lipid in membranes. (A) Representative fluorescence spectra of lipid vesicles containing 45 mol % POPC, 50 mol % POPG, and 5 mol % bisPy-PC, demonstrating an increase in the pyrene monomer signal around 380 nm paralleled with a decrease in the excimer signal around 470 nm as a result of lipid hydrolysis by PLA$_2$. The decreasing darkness of lines corresponds to the progression of time from 0 (i.e., before the addition of PLA$_2$) to 8.5 min following the addition of PLA$_2$, with 30 s intervals between consecutive spectra. (B) Activity of hIBPLA$_2$ against POPC vesicles containing POPG at mole fractions of 0, 0.1, 0.2, 0.3, 0.5, and 0.75, as indicated. PLA$_2$ activity is measured as $R_t/R_0 - 1$, where R_t and R_0 are the ratios of fluorescence intensities at 380 and 470 nm, and $R = F_{380}/F_{470}$, at time t and 0 (R_0 is R_t before the addition of PLA$_2$). The excitation was at 347 nm. The samples were contained in a buffer of 50 mM NaCl, 4 mM $CaCl_2$, 50 mM Hepes (pH 7.4), and 0.5 mM total lipid. The final concentration of PLA$_2$ was 1.7 μM, and the temperature was 25 °C. (C) Dependence of PLA$_2$ activity, determined as the initial slope of reaction progress curves shown in panel B, as a function of the mole fraction of POPG in membranes. Activities are averaged using the first three time-points at each fraction of POPG.

to the protein−membrane interface, accompanied with interface dehydration, or insertion into the membrane hydrocarbon region. Experiments with a synthetic decapeptide corresponding to the *N*-terminal helix of hIBPLA$_2$ (N10) revealed a similar dependence of λ_{max} on x_{POPG}. In both cases, λ_{max} decreased by ~10 nm as x_{POPG} increased from 0 to 1, although the absolute values of λ_{max} were considerably higher for the N10 peptide than that for hIBPLA$_2$ (Figure 1B).

Additional support for the transfer of Trp[3] of hIBPLA$_2$ and the N10 peptide from the aqueous to the membrane environment was obtained from Trp fluorescence quenching by a water-soluble quencher, acrylamide, at varying x_{POPG} values. The Stern−Volmer constant, which reflects the efficiency of fluorescence quenching, was 9.0 and 16.6 M^{-1} for the hIBPLA$_2$ and the N10 peptide free in the buffer, respectively, and decreased to 8.2 and 13.9 M^{-1}, respectively, in the presence of pure POPC vesicles and further decreased to 1.4 and 2.8 M^{-1} in a sigmoidal manner as x_{POPG} increased from 0 to 1 (Figure 2). Although these data do not clarify the question as to whether Trp[3] inserts into the membrane or becomes trapped in the protein−membrane interface, they do indicate that with increasing membrane anionic surface charge, the Trp[3], which is a part of IBS of group IB PLA$_2$s, becomes less accessible to water-soluble acrylamide.

The functional significance of the transfer of Trp[3] from water to the less polar membrane environment with increasing anionic membrane surface charge was assessed by measuring the dependence of the activity of hIBPLA$_2$ on x_{POPG}. The action of hIBPLA$_2$ on membranes containing 50 mol % POPG, 45 mol % POPC, and 5 mol % bisPy-PC resulted in a prominent increase in the pyrene monomer signal around 380 nm with a concomitant decrease in the excimer signal around 470 nm, indicating efficient phospholipid hydrolysis by hIBPLA$_2$ at $x_{POPG} = 0.5$ (Figure 3A). The activity of hIBPLA$_2$ turned out to be very sensitive to the fraction of the anionic lipid in membranes. The time dependence of lipid hydrolysis at various x_{POPG} indicated little enzyme activity at $x_{POPG} \leq 0.2$, followed by a sharp increase in PLA$_2$ activity at higher fractions of the anionic lipid, with saturation at $x_{POPG} > 0.5$ (Figure 3B,C).

hIBPLA$_2$ Significantly Penetrates into the Membrane. To determine whether the increased activity of hIBPLA$_2$ is a result of the recruitment of a larger number of the enzyme molecules to the membrane with increasing fractions of the

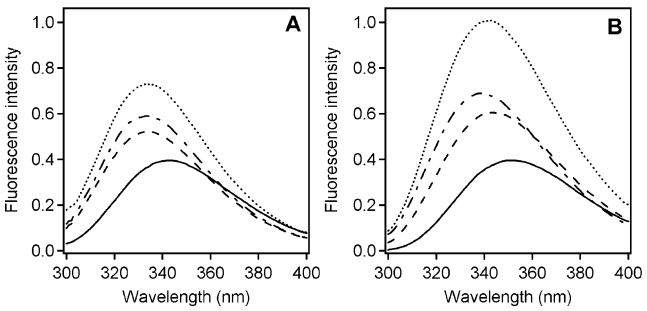

FIGURE 4: Tryptophan fluorescence quenching of hIBPLA$_2$ and the N10 peptides by water- and membrane-soluble quenchers indicates significant membrane insertion of Trp^3 in both cases. Fluorescence spectra of the hIBPLA$_2$ (A) and the N10 peptide (B) free in buffer (—), in the presence of vesicles composed of an equimolar mixture of POPC and POPG (....), in the presence of the same vesicles and 250 mM acrylamide in the buffer (.—.—.), and in the presence of vesicles containing POPC, POPG, and 10-DN at molar proportions of 4:5:1 (----). The buffer as well as the total lipid and protein (or peptide) concentrations and other experimental conditions were the same as those in Figure 1.

anionic lipid or a deeper membrane insertion of the membrane-bound enzyme, the membrane insertion of Trp^3 was directly measured by both the dual-quenching and brominated-lipid-quenching techniques. The presence of vesicles containing equal molar fractions of POPC and POPG resulted in a significant increase in Trp fluorescence intensity accompanied by a blue shift for both hIBPLA$_2$ and the N10 peptide, indicating efficient membrane binding of the molecules (Figure 4). Comparison of the quenching of Trp fluorescence by water-soluble acrylamide (250 mM in the buffer) and by membrane-soluble 10-DN (10 mol % in the membranes) allowed the determination of the dual-quenching ratios R_{DQ} = 0.60 and 0.69 for hIBPLA$_2$ and the N10 peptide, respectively, indicating insertion of Trp^3 into the hydrophobic core of the membrane.

Once it was identified that Trp^3 inserts into the membrane in the process of interfacial activation of the enzyme, it was interesting to quantitatively determine the depth of membrane insertion as well as characterize its dependence on the membrane physical properties, such as membrane surface charge and fluidity. First, the depth of insertion of Trp^3 into POPC/POPG membranes was determined for both hIBPLA$_2$ and the N10 peptide at x_{POPG} = 0.2, 0.4, and 0.75. This was done by measuring the efficiencies of Trp fluorescence quenching by Br$_2$PCs brominated at 6,7-, or 10,11-, or 11,-12-positions of the *sn*-2 acyl chains. Fluorescence spectra demonstrating the quenching of Trp^3 emission by Br$_2$PCs incorporated in vesicle membranes containing 40 mol % anionic POPG are shown in Figure 5 A and C for hIBPLA$_2$ and the N10 peptide, respectively. Analysis of these data indicated that Trp^3 penetrates into the membranes to a depth of h_m = 9.1 Å for hIBPLA$_2$ and 9.6 Å for the N10 peptide (triangles in Figure 5B and D). The data obtained on membranes containing various fractions of anionic lipid are summarized in Figure 5B and D and in Table 1 and indicate that Trp^3 inserts into POPC/POPG membranes to a depth of h_m = 9.10±0.19 Å and 9.55±0.09 Å for hIBPLA$_2$ and the N10 peptide, respectively. Determination of h_m by the Br$_2$-PC-quenching method is reliable because the bromine atoms in Br$_2$PCs brominated at 6,7-, 10,11-, or 11,12-positions have been shown by X-ray diffraction experiments to be well

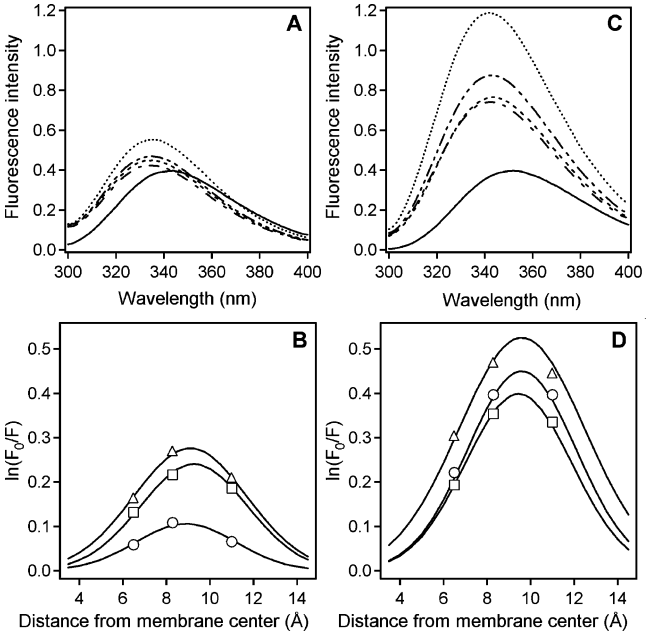

FIGURE 5: Quenching of Trp^3 fluorescence of hIBPLA$_2$ and the N10 peptide by brominated lipids allows quantitative determination of the depth of membrane insertion of the molecules. Fluorescence spectra of hIBPLA$_2$ (A) and the N10 peptide (C) free in the buffer (solid lines) in the presence of unlabeled POPC/POPG vesicles (dotted lines) and in the presence of 20 mol % Br$_2$PC in vesicles brominated at 6,7 (dashed lines), 9,10 (dashed—dotted lines), or 11,12 positions (dashed-double-dotted lines). The anionic lipid POPG was present at 40 mol %. Panels B and D show the dependencies of the efficiency of fluorescence quenching by brominated lipids as a function of the positions of bromines relative to the membrane center for hIBPLA$_2$ and the N10 peptide, respectively. Data are presented for lipid vesicles containing 20 mol % (○), 40 mol % (△), and 75 mol % (□) anionic lipid POPG. The theoretical distribution curves are simulated through eq 3. The peaks of the distribution curves correspond to the highest probability of Trp^3 location. The buffer as well as the total lipid and protein (or peptide) concentrations and other experimental conditions were the same as those in Figure 1.

Table 1: Parameters Characterizing the Insertion of hIBPLA$_2$, the N10 Peptide, hIIAPLA$_2$, and the bvPLA$_2$ into Membranes of Various Lipid Composition, as Indicated, Deduced from the Data Presented in Figures 5, 6, and 9[a]

protein	membrane	h_m (Å)	σ (Å)	S (Å)
hIBPLA$_2$	POPC + 20 mol % POPG	8.90	2.30	0.61
hIBPLA$_2$	POPC + 40 mol % POPG	9.13	2.66	1.83
hIBPLA$_2$	POPC + 75 mol % POPG	9.27	2.45	1.48
N10 peptide	POPC + 20 mol % POPG	9.60	2.50	2.82
N10 peptide	POPC + 40 mol % POPG	9.60	2.90	3.82
N10 peptide	POPC + 75 mol % POPG	9.45	2.45	2.45
hIBPLA$_2$	POPC + 50 mol % POPG	9.10	1.70	1.83
hIBPLA$_2$	DPPC + 50 mol % DPPG	13.0	3.0	0.50
hIIAPLA$_2$	POPC + 50 mol % POPG	9.50	1.43	0.52
bvPLA$_2$	POPC + 50 mol % POPG	>20	N/A	N/A

[a] The temperature was 25 °C in all cases. The meanings of parameters are explained in Materials and Methods, after eq 3.

localized at 11, 8.3, and 6.5 Å from the bilayer center, and these three Br$_2$PCs, unlike those brominated at 4,5- or 15,-16-positions, do not affect the membrane structure (*29*, 30). Within the accuracy of the estimation of h_m, which is ≤1 Å, the membrane insertion depth does not depend on the membrane surface charge. Therefore, greater PLA$_2$ activity at higher x_{POPG} values results from an increase in membrane

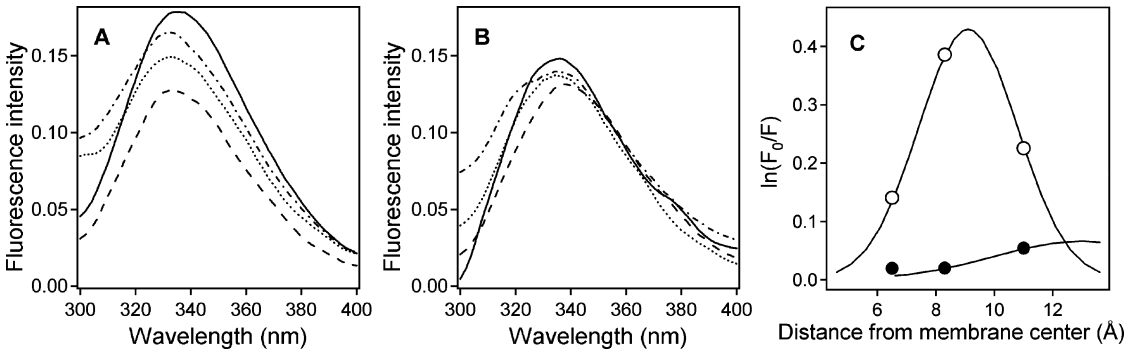

FIGURE 6: Quenching of Trp^3 fluorescence of the $hIBPLA_2$ by brominated lipids indicates significant insertion of the protein into the fluid POPC/POPG membranes but little insertion into the solid DPPC/DPPG membranes. Fluorescence spectra of $hIBPLA_2$ bound to POPC/POPG (1:1) membranes (A) or DPPC/DPPG (1:1) membranes (B) in the absence (—) and presence of 20 mol % Br_2PC in vesicles brominated at 6,7 (...), 9,10 (---), or 11,12 positions (.-.-.). Panel C shows the dependencies of the efficiency of fluorescence quenching by brominated lipids for POPC/POPG (○) and DPPC/DPPG membranes (●) as a function of the positions of bromines relative to the membrane center. The data points in panel C are obtained using fluorescence intensities at 350 nm of panels A and B. The theoretical distribution curves are simulated through eq 3. The buffer, total lipid, and protein concentrations and other experimental details are the same as those in Figure 1.

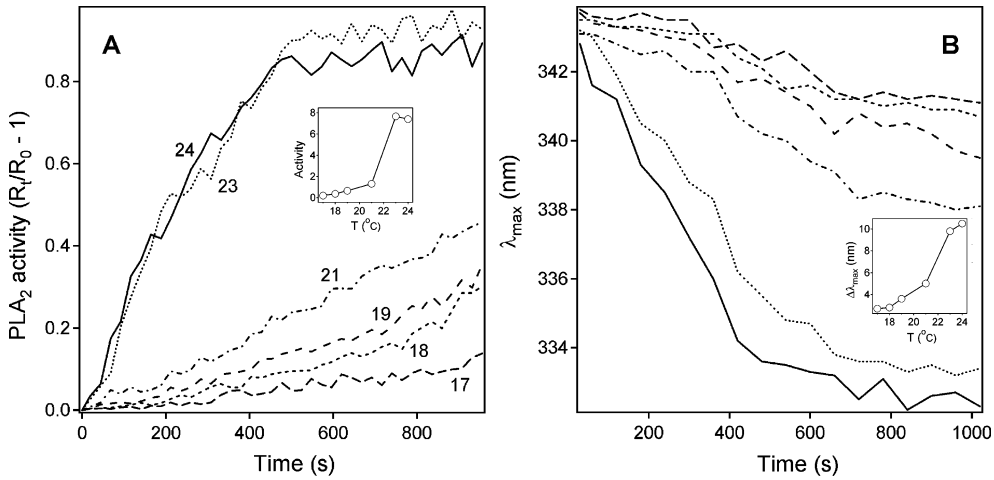

FIGURE 7: The activity of $hIBPLA_2$ sharply increases as the temperature approaches the gel-to-fluid phase transition point of the lipid, which is paralleled with an increasing blue shift of the Trp fluorescence. (A) Activity of $hIBPLA_2$ in the presence of large unilamellar DMPC vesicles containing 5 mol % bisPy-PC at different temperatures, as indicated. The method used for the measurement of PLA_2 activity and the experimental conditions were the same as those in Figure 3. The buffer was similar to that used in Figure 3, except that $CaCl_2$ concentration was 1.2 mM. Excitation was at 347 nm. The inset shows the temperature dependence of the enzyme activity; activities are obtained on the basis of the initial slopes of the curves in panel A, i.e., values of $(R_t/R_0 - 1)$ per 1 min, multiplied by a factor of 100. (B) Time dependence of the peak wavelengths (λ_{max}) of Trp emission spectra of $hIBPLA_2$ in the presence of pure DMPC vesicles, without bisPy-PC, at different temperatures (line types correspond to temperatures that are the same as those in panel A). Excitation was at 290 nm. Other experimental conditions are the same as those in A. The inset shows the temperature dependence of the change in the peak wavelength during 17 min following combination of the protein with the vesicles at specified temperatures.

recruitment of PLA_2 rather than deeper membrane insertion of the enzyme.

Membrane Insertion of hIBPLA$_2$ Is Controlled by Membrane Fluidity. The dependence of the membrane insertion of $hIBPLA_2$ on membrane fluidity was assessed by measuring Trp^3 fluorescence quenching by brominated lipids in POPC/POPG and DPPG/DPPG membranes, which are known to be in the fluid (liquid crystalline) and solid (gel) phases, respectively, at 25 °C (*9*, *32*, *33*). An analysis of the data on differential quenching of Trp^3 of $hIBPLA_2$ by Br_2-PCs indicated that Trp^3 penetrates into the fluid POPC/POPG membranes, consistent with the data described above, whereas little membrane insertion was detected for the solid DPPC/DPPG membranes (Figure 6 and Table 1). The data analysis yielded the following parameters: $h_m = 9.1$ Å, $\sigma = 1.7$ Å, and $S = 1.83$ Å for the fluid membranes, and $h_m = 13.0$ Å, $\sigma = 3.0$ Å, and S = 0.5 Å for the solid membranes (Figure 6). Significantly smaller values of S for DPPC/DPPG membranes indicate a restricted accessibility of Trp^3 to the brominated lipids in these membranes, and larger values of h_m indicate that even when the Trp^3 manages to insert into the solid DPPC/DPPG membranes, it cannot penetrate deeper than the carbonyl groups of the lipids. Also, larger values of the dispersion parameter, σ, for DPPC/DPPG membranes indicate a broader positional distribution of Trp^3 of $hIBPLA_2$ for the solid than that for the fluid membranes.

Membrane Fluidity Supports the Activity of hIBPLA$_2$. The question arises as to what the exact functional significance of membrane insertion of PLA_2 is. Does increased membrane fluidity, which facilitates membrane insertion of PLA_2, also increase the activity of the enzyme? To answer this question, the activity of $hIBPLA_2$ was measured against 1,2-dimyristoyl-*sn*-glycero-3-phosphocholine (DMPC) vesicles in a temperature range covering the gel-to-fluid phase transition of

the lipid. In separate experiments, the temperature dependence of the transfer of Trp^3 from the aqueous medium to the membrane was monitored on the basis of the blue shift of Trp emission. At 17 °C, when DMPC is in the solid (gel) phase, $hIBPLA_2$ barely showed any activity for several minutes, which was followed by a relatively low level of activity (Figure 7A). Starting at 18 °C, the lag period practically disappeared, and PLA_2 activity increased in parallel with increasing temperature, demonstrating a sigmoidal temperature dependence and reaching a maximum activity at the gel-to-fluid phase transition temperature of DMPC, $T_m \approx 23$ °C (*34*). Interestingly, the fluorescence emission spectra of Trp^3 of the protein in the presence of DMPC vesicles experienced a blue shift that was only ~2 nm at 17 °C and increased to ~10 nm in a sigmoidal manner with the phase transition of the lipid (Figure 7B). We have evaluated the effect of the lipid phase transition on membrane fluidity by measuring the temperature dependence of the generalized polarization of Laurdan incorporated in vesicle membranes at 1 mol %, as described earlier (*9*). The gel-to-fluid phase transition of the lipid was accompanied with a sharp decrease in the generalized polarization of Laurdan by ~0.7 units (not shown), indicating a substantial increase in membrane fluidity (*35*). Altogether, these data indicate that an increase in membrane fluidity results in the membrane insertion of $hIBPLA_2$, which is paralleled with substantial enhancement in PLA_2 activity, suggesting that membrane insertion may be required for the activity of at least this PLA_2 isoform.

Membrane Insertion of PLA_2s Is Isoform-Specific. Having established that $hIBPLA_2$ considerably penetrates into the fluid membranes, we asked the question whether this property is shared by other PLA_2 isoforms. Membrane insertion was studied for two additional PLA_2 isoforms, one of which (V3W-$hIIAPLA_2$) shares 40% sequence identity with $hIBPLA_2$ and has very similar 3-D structure, and the other ($bvPLA_2$) shares little sequence homology with $hIBPLA_2$ and has significantly different structure. The $bvPLA_2$ is a 134-residue group III secretory PLA_2 and has two tryptophans at positions 8 and 128. We used the V3W mutant of $hIIAPLA_2$ because the wild-type enzyme has no tryptophans but has eight tyrosines that are spread all over the protein molecule and, therefore, cannot be used for the determination of membrane insertion by the fluorescence-quenching technique. Replacement of Val^3 by Trp yields a suitable homologue for this purpose. Although we clearly realized that the membrane-binding properties of the V3W mutant may not precisely correspond to those of the wild-type enzyme, it was still interesting to see how structural similarities (or dissimilarities) determine the membrane insertion properties of PLA_2s.

First, the membrane insertion of both proteins was evaluated by the dual quenching method. The peak of Trp fluorescence of the V3W-$hIIAPLA_2$ free in buffer was located at 347−348 nm and experienced a 8−9 nm blue shift, accompanied by an increase in intensity, in the presence of POPC/POPG (1:1) membranes (Figure 8A). For the V3W-$hIIAPLA_2$, Trp emission was quenched more strongly by the membrane-soluble 10-DN than that by the water-soluble acrylamide, yielding $R_{DQ} = 0.78$. However, Trp fluorescence spectra of the free $bvPLA_2$ were centered at 339−340 nm, and the presence of POPC/POPG (1:1) membranes resulted only in an increase in the emission intensity without any

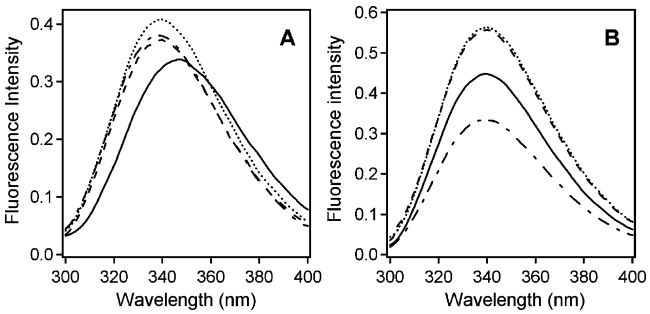

FIGURE 8: Tryptophan fluorescence quenching of V3W-$hIIAPLA_2$ and $bvPLA_2$ by water- and membrane-soluble quenchers indicates significant membrane insertion of Trp^3 of V3W-$hIIAPLA_2$ and no insertion of tryptophans of $bvPLA_2$. Fluorescence spectra of the V3W-$hIIAPLA_2$ (A) and $bvPLA_2$ (B) free in buffer (—), in the presence of vesicles composed of an equimolar mixture of POPC and POPG (....), in the presence of the same vesicles and 250 mM acrylamide in the buffer (.—.—.), and in the presence of vesicles containing POPC, POPG, and 10-DN at molar proportions of 4:5:1 (----). The buffer as well as the total lipid and protein concentrations and other experimental conditions were the same as those in Figure 1.

blue shift (Figure 8B). In this case, Trp emission was strongly quenched by acrylamide, whereas quenching by 10-DN was negligible, resulting in $R_{DQ} = 62.3$ (Figure 8B). This is a clear message that whereas Trp^3 of the V3W-$hIIAPLA_2$ penetrates into the POPC/POPG membranes, none of the two tryptophans of $bvPLA_2$ do so.

A quantitative evaluation of the membrane insertion of tryptophans of V3W-$hIIAPLA_2$ and $bvPLA_2$ indicated that the Trp^3 of V3W-$hIIAPLA_2$ was quenched by all three brominated lipids in membranes containing 40 mol % POPG, 40 mol % POPC, and 20 mol % Br_2PC. The stronger quenching was achieved in the presence of 9,10-Br_2PC (Figure 9A), and the data were consistent with membrane insertion of Trp^3 to a depth of 9.5 Å from the membrane center (Figure 9C and Table 1). In contrast, tryptophans of $bvPLA_2$ were not quenched by any of the Br_2PCs (Figure 9B). To provide more evidence for the absence of fluorescence quenching of $bvPLA_2$ by brominated lipids, experiments were carried out with membranes containing 20, 40, and 75 mol % POPG. In no case was any significant fluorescence quenching detected (Figure 9C). The fact that the tryptophans of $bvPLA_2$ are not even quenched by 6,7-Br_2PC indicates that they are separated from the bromines of this lipid (11 Å from the membrane center) at least by the radius of action of Br quenching, which was estimated to be 9 Å (*36*). In other words, the tryptophans of $bvPLA_2$ are located at least 20 Å away from the membrane center, that is, above the phosphate groups of membrane phospholipids.

DISCUSSION

While membrane insertion appears to be an important aspect of the function of peripheral membrane proteins, the question as to whether secretory PLA_2s partially insert into membranes in the process of interfacial activation is still a subject of debate. Given this background, the aim of this work has been to establish the membrane insertion of PLA_2s, to characterize the dependence of membrane insertion on the membrane surface charge and fluidity, to identify the functional significance for membrane insertion, and to

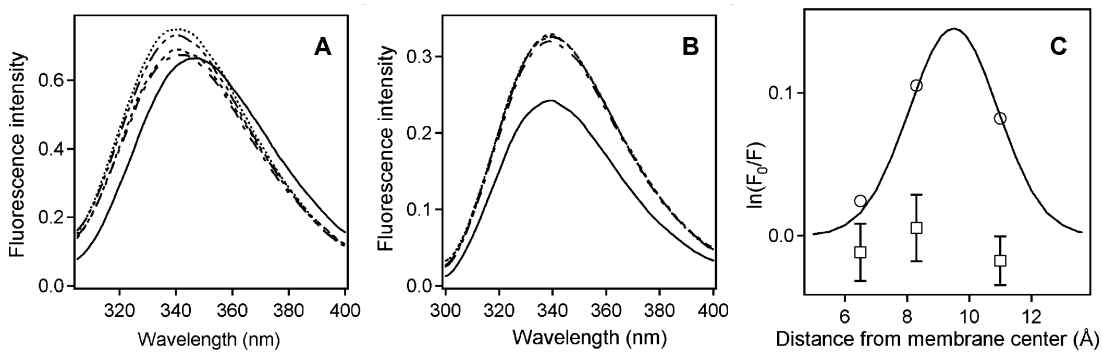

FIGURE 9: Quenching of tryptophan fluorescence of the V3W-hIIAPLA$_2$ and bvPLA$_2$ by brominated lipids allows the determination of the depth of membrane insertion of Trp[3] of V3W-hIIAPLA$_2$ and confirms that the tryptophans of bvPLA$_2$ do not insert into the hydrocarbon region of the membrane. Fluorescence spectra of V3W-hIIAPLA$_2$ (A) and bvPLA$_2$ (B) free in the buffer (solid lines), in the presence of unlabeled vesicles containing POPC and 40 mol % POPG (dotted lines), and in the presence of 20 mol % Br_2PC in vesicles brominated at 6,7 (dashed lines), 9,10 (dashed−dotted lines), or 11,12 positions (dashed-double-dotted lines). In ternary membranes, both POPC and POPG are present at 40 mol %, and the rest is Br_2PC. Panel C shows the dependencies of the efficiency of fluorescence quenching of V3W-hIIAPLA$_2$ (○) and bvPLA$_2$ (□) by brominated lipids as a function of the positions of bromines relative to the membrane center. In the case of bvPLA$_2$, the average data are shown that were obtained for membranes containing 20, 40, or 75% anionic lipid and POPG, along with the standard deviations. The theoretical distribution curve for V3W-hIIAPLA$_2$ is simulated through eq 3. The buffer as well as the total lipid and protein concentrations and other experimental conditions were the same as those in Figure 1.

determine if membrane insertion of PLA$_2$s is isoform-specific.

The blue shift of Trp[3] fluorescence of hIBPLA$_2$ and reduced quenching by acrylamide at higher fractions of POPG in membranes (Figures 1 and 2) obviously reflects increased membrane recruitment of the cationic protein because of electrostatic interactions, which in turn results in a greater overall PLA$_2$ activity (Figure 3). These data are consistent with earlier reports that surface electrostatics plays a major role in membrane binding and activity of group I/II PLA$_2$s (*15*, *16*, *24*, *37*, *38*).

Our data indicate that hIBPLA$_2$ significantly inserts into membranes. Membrane insertion properties of hIBPLA$_2$ and its *N*-terminal helix, that is, the N10 peptide, demonstrate remarkable similarities (Figures 1, 2, 4, and 5 and Table 1), which is in line with our earlier findings that the *N*-terminal helix is an important determinant of the membrane-binding mode of hIBPLA$_2$ (*6*, *24*). Membrane insertion of hIBPLA$_2$ is facilitated by increased membrane fluidity, as demonstrated by efficient penetration into the fluid POPC/POPG membranes but not into the solid DPPC/DPPG membranes (Figure 6). However, PLA$_2$ activity against DMPC vesicles sharply increases as the temperature approaches the gel-to-fluid phase transition temperature of the lipid (Figure 7A), which suggests a correlation between membrane fluidity and PLA$_2$ activity. The increase in the activity of hIBPLA$_2$ at temperatures close to T_m is paralleled with an increasing blue shift of Trp[3] (Figure 7B). This might result from either the membrane binding of a larger number PLA$_2$ molecules or deeper membrane insertion of the same fraction of membrane-bound PLA$_2$s. Although our data present clear evidence for deeper membrane insertion of PLA$_2$ with increasing membrane fluidity, the question still remains as to whether membrane fluidity also enhances the membrane binding of PLA$_2$ that contributes to an overall higher enzyme activity. Because hydrolysis of membrane lipids results in gradual accumulation of reaction products (lyso-phospholipid and fatty acid) in membranes, which continuously modulate the properties of vesicles, including the fluidity, size, morphology, surface charge, and phase separation (*39*, *40*), it is difficult to explicitly determine the dependence of PLA$_2$ activity on membrane fluidity under otherwise invariable conditions.

Earlier articles on relationships between lipid phase transitions, PLA$_2$ binding, and activity appear to be complicated. Jain et al. (*41*) reported that pIBPLA$_2$, unlike a cobra venom (group IA) PLA$_2$, did not bind to the ditetradecyl-PC membranes at temperatures below or above T_m but did bind to membranes over a wide temperature range when reaction products (lyso-PC and fatty acid) were added. The activity of pIBPLA$_2$ against DPPC vesicles increased close to the T_m of the lipid, and the enzyme activity was substantially higher against POPC than that against DPPC vesicles at all temperatures tested (*42*). These data were thought to reflect an easier penetration of the enzyme into more fluid membranes and directly support our results and interpretation of the membrane fluidity dependence of insertion and activity of hIBPLA$_2$.

The gel-to-fluid phase transition of PC membranes causes a 30−40% decrease in lipid-packing density (*43*−*45*), a 2−4-fold reduction in the membrane microviscosity (*46*, *47*) and a 2-fold increase in hydration (*48*). The lateral expansion and reduced microviscosity of the membrane at $T > T_m$ would facilitate membrane insertion of molecules but increased hydration would resist intimate physical contacts. The well-established trend is that membrane fluidization in most cases increases the binding and insertion of various molecules (*49*−*54*), indicating that the looser lipid packing and lower viscosity are perhaps the dominant factors. Consistent with this, Van der Wiele et al. (*55*) have found that "pancreatic PLA$_2$ cannot penetrate into the densely packed bilayer structures" and demonstrated enhanced membrane anchoring of pIBPLA$_2$ following covalent modification by fatty acids. Also, the lag time preceding efficient hydrolysis of lipid monolayers at the air−water interface by pIBPLA$_2$ decreased from ∼60 min to 0 as the monolayer surface pressures decreased form 20 to 8 mN/m (*56*), which likely indicates an easier penetration of PLA$_2$ into more loosely packed monolayers.

In conjunction with earlier findings, our results indicate that membrane surface charge and membrane fluidity play distinctly different roles in PLA$_2$−membrane interactions.

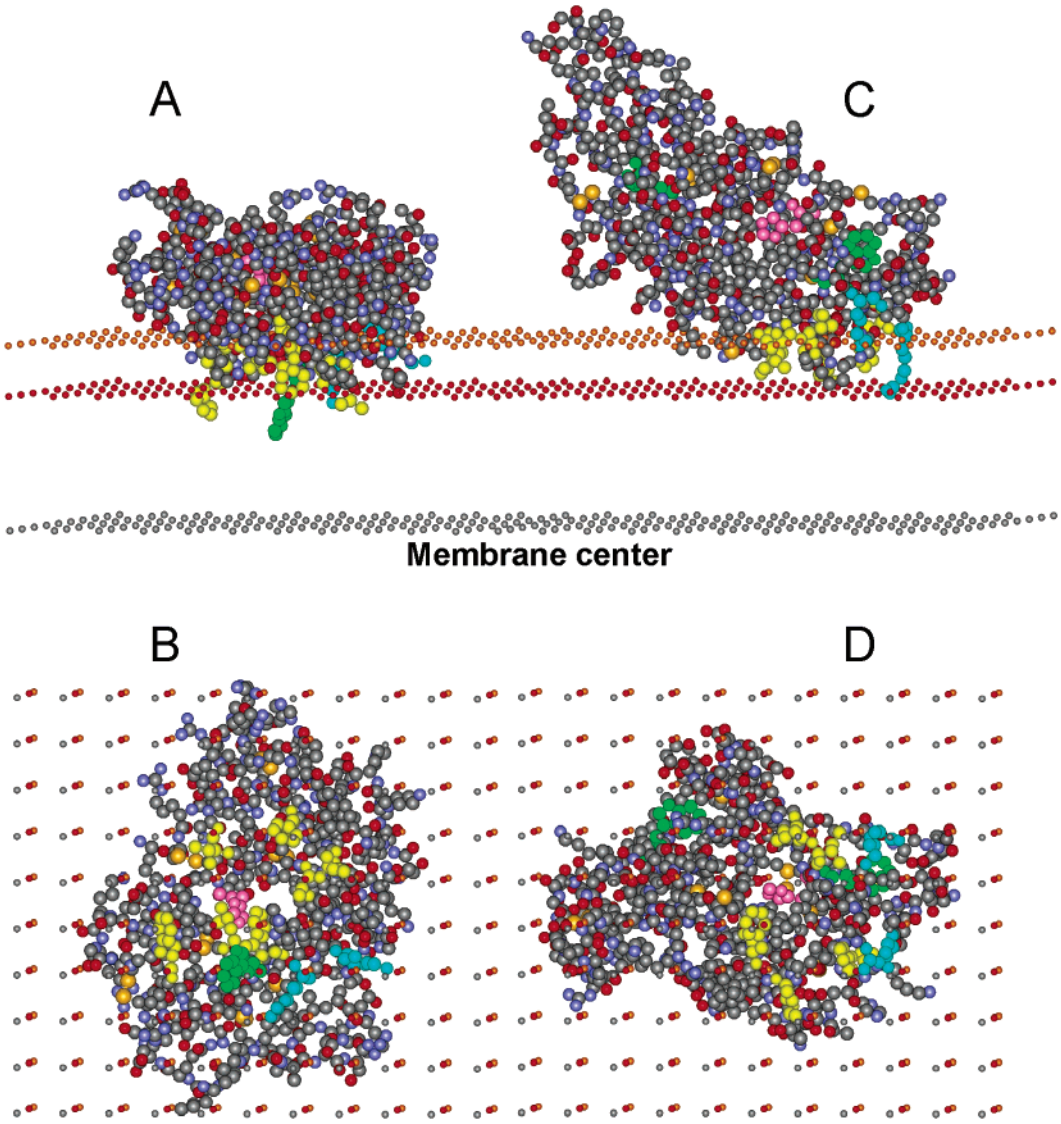

FIGURE 10: Models for the membrane binding of V3W-hIIAPLA$_2$ (A and B) and bvPLA$_2$ (C and D), as viewed from the side (A and C) and from the membrane center (B and D). The structure of V3W-hIIAPLA$_2$ was homology modeled by SWISS-MODEL (*61*), using the hIIAPLA$_2$ structure (pdb entry 1N29) as a template, and the bvPLA$_2$ structure is based on pdb entry 1POC. Proteins are shown in CPK (Corey−Pauling−Kulton) format, without hydrogens. Atoms are colored according to convention: carbons, gray; nitrogens, blue; oxygens, red; and sulfur atoms, gold. In both cases, the catalytic histidine is colored magenta, the hydrophobic residues surrounding the substrate-binding cleft and involved in membrane anchoring (Leu^2, Ala^{18}, Leu^{19}, Phe^{23}, Val^{30}, Phe^{63} in the case of V3W-hIIAPLA$_2$ and Ile^1, Ile^2, Phe^{24}, Ile^{78}, Phe^{82} for bvPLA$_2$) are colored yellow, and the cationic residues that support membrane binding by ionic and/or H-bonding interactions with the lipid polar groups (Arg^7 and Lys^{10} for V3W-hIIAPLA$_2$ and Lys^{14} and Arg^{23} for bvPLA$_2$) are colored light blue. Trp^3 of V3W-hIIAPLA$_2$ and Trp^8 and Trp^{128} of bvPLA$_2$ are colored green. The three layers of nonprotein atoms are introduced to schematically show membrane sections corresponding to the acyl chain terminal methyl carbons (gray), the *sn*-1 carbonyl oxygens (red), and the phosphorus atoms (orange) of membrane phospholipids. The *z*-coordinates of these layers are 0, 14.5, and 20 Å, respectively. Note that the catalytic His^{47} of V3W-hIIAPLA$_2$ is hidden in the protein body (A) and is only accessible from the membrane (B), whereas the catalytic His^{34} of bvPLA$_2$ is open both to the aqueous phase (C) and to the membrane (D). The cavity leading to His^{34} in panel C is flanked by side chains of Thr^{57} and Asp^{35} from the left and the right is ~7 Å wide horizontally and is much wider in the vertical dimension.

The role of the membrane surface charge is evidently to increase the strength of membrane binding of PLA$_2$ because of enhanced electrostatic interactions, which determines the fluorescence blue shift and increased PLA$_2$ activity at higher fractions of POPG in membranes (Figures 1−3). The role of membrane fluidity is probably to facilitate an optimal mode of membrane binding of PLA$_2$ by inserting certain nonpolar residues into the membrane hydrocarbon core. However, this may be required only for those PLA$_2$ isoforms that do penetrate below the carbonyl groups of lipids in order to perform their function, which appears not to be a common feature across PLA$_2$ isoforms. Our data indeed demonstrate that the structurally similar hIBPLA$_2$ and V3W-hIIAPLA$_2$ considerably penetrate into the hydrocarbon core of membranes, but the structurally diverse bvPLA$_2$ does not. The latter is in accordance with earlier findings of a peripheral mode of membrane binding of bvPLA$_2$ (*12*). The nonpolar amino acid residues that constitute the bulk of the IBS of bvPLA$_2$ have been proposed to be located at the lipid headgroup region of the membrane and to facilitate protein−membrane H bonding via a surface dehydration mechanism (*13*, *57*). Detailed studies on the membrane fluidity dependence of membrane insertion and activity of various isoforms of PLA$_2$s are currently in progress in our lab. As shown in

the accompanying article (*25*), the hIIAPLA$_2$ demonstrates little activity against PC membranes in the gel phase and high activity at temperatures close to T_m, resembling the behavior of hIBPLA$_2$ (Figure 7). The activity of bvPLA$_2$, however, appears to be less sensitive to membrane fluidity. When the *sn*-1 chain of dioleoyl-PC was replaced by a palmitic or a stearic acid residue, making the membranes more rigid, the activity of pIBPLA$_2$ decreased by 51% and 65%, whereas that of bvPLA$_2$ decreased by only 8% and 32%, respectively (*42*). The authors mentioned that "the phenomenon of bilayer penetration may be linked to the concept of interfacial activation" (*42*). We agree with this conjecture and think that the emerging evidence of the distinct modes of membrane binding of different PLA$_2$ isoforms may indicate specific modes of substrate acquisition and product release, as developed below.

Gelb et al. (*10*) discussed distinct mechanisms of interfacial activation and substrate accession of membrane binding enzymes, which were classified into two types, interfacial (IF) and noninterfacial (NIF). Both function in a membrane-bound form but acquire the substrate from the membrane or from the aqueous phase, respectively. In addition, both types may undergo allosteric conformational changes upon membrane-induced interfacial activation, corresponding to interfacial with interfacial activation (IF-IFA) and noninterfacial with interfacial activation (NIF-IFA) enzymes. Secretory PLA$_2$s have been classified into the interfacial enzymes, albeit without the specification of isoforms (*10*). Given the strong experimental evidence that at least group IB and IIA PLA$_2$s undergo allosteric conformational changes during interfacial activation (refs 6, 24, and 59−60 and references therein), these molecules should belong to the class of IF-IFA enzymes. In a process of interfacial activation, they bind to the target membrane and acquire the phospholipid substrate from the membrane.

The more superficial membrane-binding mode of bvPLA$_2$ (ref 12 and this work) suggests that this PLA$_2$ isoform may employ a different strategy of action. An inspection of the 3-D structures of V3W-hIIAPLA$_2$ and bvPLA$_2$ indicates that although the catalytic His^{47} of V3W-hIIAPLA$_2$ is efficiently hidden inside the protein body and is accessible only from the substrate-binding cleft, the catalytic His^{34} of bvPLA$_2$ is accessible both from the IBS and from the aqueous phase through a cavity of considerable dimension. This information, combined with the present data on the distinct modes of membrane binding of group I/II and group III PLA$_2$s, led us to construct the models of membrane-bound V3W-hIIAPLA$_2$ and bvPLA$_2$, as shown in Figure 10. The nonpolar and cationic residues of V3W-hIIAPLA$_2$ and bvPLA$_2$ that make intimate contacts with the membrane (Figure 10 legend) are consistent with earlier data (*12*−*14*, *57*). The models of Figure 10 suggest that bvPLA$_2$ may access either the membrane-residing or aqueous-phospholipid substrate. Alternatively, the substrate may be acquired from the membrane and hydrolyzed, and then both or one of the products may be released into the aqueous phase using the cavity seen in Figure 10C. This opening is gated by the side chains of Thr^{57} and Asp^{35} and is ∼7 Å wide, indicating that the cavity would allow the entrance or release of a lipid molecule. Therefore, the activity of bvPLA$_2$ is likely to be less sensitive to membrane binding, which would make it a less typical interfacial enzyme. More specifically, bvPLA$_2$ may represent an intermediate case of interfacial and noninterfacial enzymes, which may function in the membrane-bound state but can acquire the substrate both from the membrane and from the aqueous phase. These considerations suggest that isoform-specific differences in membrane-binding modes are likely to be related to significant mechanistic differences between group I/II and group III PLA$_2$s. Further studies on substrate concentration dependence and temperature dependence of membrane insertion and the activities of these and other PLA$_2$ isoforms will shed more light on the molecular mechanisms of these much studied but still largely enigmatic enzymes.

REFERENCES

1. Bottomlay, M. J., Salim, K., and Panayotou, G. (1998) Phospholipid-binding protein domains, *Biochim. Biophys. Acta 1436*, 165−183.
2. DiNitto, J. P., Cronin, T. C., and Lambright, D. G. (2003) Membrane recognition and targeting by lipid-binding domains, Science's stke, www.stke.org/cgi/content/full/sigtrans;2003/213/re16.
3. Nielsen, R. D., Che, K., Gelb, M. H., and Robinson, B. H. (2005) A ruler for determining the position of proteins in membranes, *J. Am. Chem. Soc. 127*, 6430−6442.
4. Malmberg, N. J., and Falke, J. J. (2005) Use of EPR power saturation to analyze the membrane-docking geometries of peripheral proteins: applications to C2 domains, *Annu. Rev. Biophys. Biomol. Struct. 34*, 71−90.
5. Tatulian, S. A., Qin, S., Pande, A. H., and He, X. (2005) Positioning membrane proteins by novel protein engineering and biophysical approaches, *J. Mol. Biol. 351*, 939−947.
6. Qin, S., Pande, A. H., Nemec, K. N., He, X., and Tatulian, S. A. (2005) Evidence for the regulatory role of the N-terminal helix of secretory phospholipase A_2 from studies on native and chimeric proteins, *J. Biol. Chem. 280*, 36773−36783.
7. Kutateladze, T. G., Capelluto, D. G. S., Ferguson, C. G., Cheever, M. L., Kutateladze, A. G., Prestwich, G. D., and Overduin, M. (2004) Multivalent mechanism of membrane insertion by the FYVE domain, *J. Biol. Chem. 279*, 3050−3057.
8. Rufener, E., Frazier, A. A., Wieser, C. M., Hinderliter, A., and Cafiso, D. S. (2005) Membrane-bound orientation and position of the synaptotagmin C2B domain determined by site-directed spin labeling, *Biochemistry 44*, 18−28.
9. Pande, A. H., Qin, S., and Tatulian, S. A. (2005) Membrane fluidity is a key modulator of membrane binding, insertion, and activity of 5-lipoxygenase, *Biophys. J. 88*, 4084−4094.
10. Gelb, M. H., Min, J.-H., and Jain, M. K. (2000) Do membrane-bound enzymes access their substrates from the membrane or aqueous phase: interfacial versus non-interfacial enzymes, *Biochim. Biophys. Acta 1488*, 20−27.
11. Scott, D. L., White, S. P., Otwinowski, Z., Yuan, W., Gelb, M. H., and Sigler, P. B. (1990) Interfacial catalysis: the mechanism of phospholipase A_2, *Science 250*, 1541−1546.
12. Lin, Y., Nielsen, R., Murray, D., Hubbell, W. L., Mailer, C., Robinson, B. H., and Gelb, M. H. (1998) Docking phospholipase A_2 on membranes using potential-modulated spin relaxation magnetic resonance, *Science 279*, 1925−1929.
13. Bollinger, J. G., Diraviyam, K., Ghomashchi, F., Murray, D., and Gelb, M. H. (2004) Interfacial binding of bee venom secreted phospholipase A_2 to membranes occurs predominantly by a nonelectrostatic mechanism, *Biochemistry 43*, 13293−13304.
14. Canaan, S., Nielsen, R., Ghomashchi, F., Robinson, B. H., and Gelb, M. H. (2002) Unusual mode of binding of human group IIA secreted phospholipase A_2 to anionic interfaces as studied by continuous wave and time domain electron paramagnetic resonance spectroscopy, *J. Biol. Chem. 277*, 30984−30990.
15. Diraviyam, K., and Murray, D. (2006) Computational analysis of the membrane association of group IIA secreted phospholipases A_2: a differential role for electrostatics, *Biochemistry 45*, 2584−2598.
16. Volwerk, J. J., Jost, P. C., de Haas, G. H., and Griffith, O. H. (1986) Activation of porcine pancreatic phospholipase A_2 by the

presence of negative charge at the lipid-water interface, *Biochemistry 25*, 1726−1733.
17. Zhou, F., and Schilten, K. (1996) Molecular dynamics study of phospholipase A_2 on a membrane surface, *Proteins: Struct., Funct., Genet. 25*, 12−27.
18. Vacklin, H. P., Tiberg, F., Fragneto, G., and R. K. Thomas (2005) Phospholipase A_2 hydrolysis of supported phospholipid bilayers: a neutron reflectivity and ellipsometry study, *Biochemistry 44*, 2811−2821.
19. Jain, M. K., and Maliwal, B. P. (1985) The environment of tryptophan in pig pancreatic phospholipase A_2 bound to bilayers, *Biochim. Biophys. Acta 814*, 135−140.
20. Jain, M. K., and Maliwal, B. P. (1993) Spectroscopic properties of the states of pig pancreatic phospholipase A_2 at interfaces and their possible molecular origin, *Biochemistry 32*, 11838−11846.
21. Jain, M. K., and Vaz, W. L. C. (1987) Dehydration of the lipid−protein microinterface on binding of phospholipase A_2 to lipid bilayers, *Biochim. Biophys. Acta 905*, 1−8.
22. Yu, B. Z., Janssen, M. J. W., Verheij, H. M., and Jain, M. K. (2000) Control of the chemical step by leucine-31 of pancreatic phospholipase A_2, *Biochemistry 39*, 5702−5711.
23. Bahnson, B. J. (2005) Structure, function and interfacial allosterism in phospholipase A_2: insight from the anion-assisted dimer, *Arch. Biochem. Biophys. 433*, 96−106.
24. Qin, S., Pande, A. H., Nemec, K. N., and Tatulian, S. A. (2004) The N-terminal α-helix of pancreatic phospholipase A_2 determines productive-mode orientation of the enzyme at the membrane surface, *J. Mol. Biol. 344*, 71−89.
25. Nemec, K. N., Pande, A. H., Qin, S., Bieber Urbauer, R. J., Tan, S., Moe, D. and Tatulian, S. A. (2006) Structural and functional effects of tryptophans inserted into the membrane-binding and substrate-binding sites of human group IIA phospholipase A_2, *Biochemistry 45*, pp 12448−12460.
26. Lakowicz, J. R. (1999) *Principles of Fluorescence Spectroscopy*, 2nd ed., Kluwer Academic/Plenum Publishers, New York.
27. Caputo, G. A., and London, E. (2003) Using a novel dual fluorescence quenching assay for measurement of tryptophan depth within lipid bilayers to determine hydrophobic α-helix locations within membranes, *Biochemistry 42*, 3265−3274.
28. Caputo, G. A., and London, E. (2004) Position and ionization state of Asp in the core of membrane-inserted alpha helices control both the equilibrium between transmembrane and nontransmembrane helix topography and transmembrane helix positioning, *Biochemistry 43*, 8794−8806.
29. McIntosh, T. J., and Holloway, P. W. (1987) Determination of the depth of bromine atoms in bilayers formed from bromolipid probes, *Biochemistry 26*, 1783−1788.
30. Ladokhin, A. S. (1997) Distribution analysis of depth-dependent fluorescence quenching in membranes: a practical guide, *Methods Enzymol. 278*, 462−473.
31. London, E., and Ladokhin, A. S. (2002) Measuring the depth of amino acid residues in membrane-inserted peptides by fluorescence quenching, *Curr. Top. Membr. 52*, 89−115.
32. Stubbs, C. D., Kouyama, T., Kinosita, K., and Ikegami, A. (1981) Effect of double bonds on the dynamic properties of the hydrocarbon region of lecithin bilayers, *Biochemistry 20*, 4257−4262.
33. Litman, B. J., Lewis, E. N., and Levin. I. W. (1991) Packing characteristics of highly unsaturated bilayer lipids: Raman spectroscopic studies of multilamellar phosphatidylcholine dispersions, *Biochemistry 30*, 313−319.
34. Sturtevant, J. M. (1984) The effects of water-soluble solutes on the phase transitions of phospholipids, *Proc. Natl. Acad. Sci. U.S.A. 81*, 1398−1400.
35. Harris, F. M., Best, K. B., and Bell, J. D. (2002) Use of laurdan fluorescence intensity and polarization to distinguish between changes in membrane fluidity and phospholipid order, *Biochim. Biophys. Acta 1565*, 123−128.
36. Bolen, E. J., and Holloway, P. W. (1990) Quenching of tryptophan fluorescence by brominated phospholipid, *Biochemistry 29*, 9638−9643.
37. Bezzine, S., Bollinger, J. G., Singer, A. G., Veatch, S. L., Keller, S. L., and Gelb, M. H. (2002) On the binding preference of human groups IIA and X phospholipases A_2 for membranes with anionic phospholipids, *J. Biol. Chem. 277*, 48523−48534.
38. Gadd, M. E., and Biltonen, R. L. (2000) Characterization of the interaction of phospholipase A_2 with phosphatidylcholine-phosphatidylglycerol mixed lipids, *Biochemistry 39*, 9623−9631.
39. Burack, W. R., Dibble, A. R., Allietta, M. M., and Biltonen, R. L. (1997) Changes in vesicle morphology induced by lateral phase separation modulate phospholipase A_2 activity, *Biochemistry 36*, 10551−10557.
40. Sanchez, S. A., Bagatolli, L. A., Gratton, E., and Hazlett, T. L. (2002) A two-photon view of an enzyme at work: *Crotalus atrox* venom PLA_2 interaction with single-lipid and mixed-lipid giant unilamellar vesicles, *Biophys. J. 82*, 2232−2243.
41. Jain, M. K., Egmond, M. R., Verheij, H. M., Apitz-Castro, R., Dijkman, R., and de Haas, G. H. (1982) Interaction of phospholipase A_2 and phospholipid bilayers, *Biochim. Biophys. Acta 688*, 341−348.
42. Kinkaid, A., and Wilton, D. C. (1991) Comparison of the catalytic properties of phospholipase A_2 from pancreas and venom using a continuous fluorescence displacement assay, *Biochem. J. 278*, 843−848.
43. Seddon, J. M., and Cevc, G. (1993) Lipid Polymorphism: Structure and Stability of Lyotropic Mesophases of Phospholipids, in *Phospholipids Handbook* (Cevc, G., Ed.) pp 403−454, Marcel Dekker, New York.
44. Xiang, T. X., and Anderson, B. D. (1997) Permeability of acetic acid across gel and liquid-crystalline lipid bilayers conforms to free-surface-area theory, *Biophys. J. 72*, 223−237.
45. Sum, A. K., Faller, R., and de Pablo, J. J. (2003) Molecular simulation study of phospholipid bilayers and insights of the interactions with disaccharides, *Biophys. J. 85*, 2830−2844.
46. Cevc, G. (1993) Solute Transport Across Bilayers, in *Phospholipids Handbook* (Cevc, G., Ed.) pp 639−661, Marcel Dekker, New York.
47. Bahri, M. A., Heyne, B. J., Hans, P., Seret, A. E., Mouithys-Mickalad, A. A., and Hoebeke, M. D. (2005) Quantification of lipid bilayer effective microviscosity and fluidity effect induced by propofol, *Biophys. Chem. 114*, 53−61.
48. McIntosh, T. J., and Magid, A. D. (1993) Phospholipid Hydration, in *Phospholipids Handbook* (Cevc, G., Ed.) pp 553−577, Marcel Dekker, New York.
49. Tatulian, S. A. (1983) Effect of lipid phase transition on the binding of anions to dimyristoylphosphatidylcholine liposomes, *Biochim. Biophys. Acta 736*, 189−195.
50. Demura, M., Kamo, N., and Kobatake, Y. (1987) Binding of lipophilic cations to the liposomal membrane: thermodynamic analysis, *Biochim. Biophys. Acta 903*, 303−308.
51. Langner, M., and Hui, S. W. (1993) Merocyanine interaction with phosphatidylcholine bilayers, *Biochim. Biophys. Acta 1149*, 175−179.
52. Lande, M. B., Donovan, J. M., and Zeidel, M. L. (1995) The relationship between membrane fluidity and permeabilities to water, solutes, ammonia, and protons, *J. Gen. Physiol. 106*, 67−84.
53. Taylor, K. M., and Roseman, M. A. (1996) Effect of cholesterol on the tight insertion of cytochrome b5 into large unilamellar vesicles, *Biochim. Biophys. Acta 1278*, 35−40.
54. Pezeshk, A., Wojas, J., and Subczynski, W. K. (1998) Partitioning and structural effects of the antitumor drug daunomycin on model membranes, *Life Sci. 63*, 1863−1870.
55. Van der Wiele, F. C., Atsma, W., Roelofsen, B., van Linde, M., Van Binsbergen, J., Radvanyi, F., Raykova, D., Slotboom, A. J., and de Haas, G. H. (1988) Site-specific ϵ-NH_2 monoacylation of pancreatic phospholipase A_2. 2. Transformation of soluble phospholipase A_2 into a highly penetrating "membrane-bound" form, *Biochemistry 27*, 1688−1694.
56. Cajal, Y., Berg, O. G., and Jain, M. K. (2004) Origins of delays in monolayer kinetics: phospholipase A_2 paradigm, *Biochemistry 43*, 9256−9264.
57. Ghomashchi, F., Lin, Y., Hixon, M. S., Yu, B.-Z., Annand, R., Jain, M. K., and Gelb, M. H. (1998) Interfacial recognition by bee venom phospholipase A_2: insights into nonelectrostatic molecular determinants by charge reversal mutagenesis, *Biochemistry 37*, 6697−6710.
58. Berg, O. G., Rogers, J., Yu, B.-Z., Yao, J., Romsted, L. S., and Jain, M. K. (1997) Thermodynamic and kinetic basis of interfacial activation: resolution of binding and allosteric effects on pancreatic phospholipase A2 at zwitterionic interfaces, *Biochemistry 36*, 14512−14530.
59. Berg, O. G., Yu, B.-Z., Chang, C., Koehler, K. A., and Jain, M. K. (2004) Cooperative binding of monodisperse anionic amphiphiles to the i-face: phospholipase A_2-paradigm for interfacial binding, *Biochemistry 43*, 7999−8013.

60. Tatulian, S. A. (2001) Toward understanding interfacial activation of secretory phospholipase A_2 (PLA_2): membrane surface properties and membrane-induced structural changes in the enzyme contribute synergistically to PLA_2 activation, *Biophys. J. 80*, 789−800.

61. Schwede, T., Kopp, J., Guex, N., and Peitsch, M. C. (2003) SWISS-MODEL: An automated protein homology-modeling server. *Nucleic Acids Res. 31*, 3381−3385.

BI060898Q